Biofuel Research Journal 35 (2022) 1648-1658

Biofuel Research Journal

Journal homepage: www.biofueljournal.com

Original Research Paper

Beyond conventional biomass valorisation: pyrolysis-derived products for biomedical applications

Mohd Amir Asyraf Mohd Hamzah[1], Rosnani Hasham[1], Nik Ahmad Nizam Nik Malek[2], Zanariah Hashim[1], Maizatulakmal Yahayu[3], Fazira Ilyana Abdul Razak[4], Zainul Akmar Zakaria[1,*]

[1]*School of Chemical and Energy Engineering, Faculty of Engineering, Universiti Teknologi Malaysia, 81310 Johor Bahru, Johor, Malaysia.*

[2]*Department of Biosciences, Faculty of Science, Universiti Teknologi Malaysia, 81310 Johor Bahru, Johor, Malaysia.*

[3]*Institute of Bioproduct Development, Universiti Teknologi Malaysia, 81310 Johor Bahru, Johor, Malaysia.*

[4]*Department of Chemistry, Faculty of Science, Universiti Teknologi Malaysia, 81310 Johor Bahru, Johor, Malaysia.*

HIGHLIGHTS

- Acid condensate obtained by pyrolysis of palm kernel shells showed potential biomedical application.
- Combined fraction acid condensate 3 (CFAC-3) exhibited high antioxidant activity.
- CFAC-3 exhibited no cytotoxicity at ≤50 µg/mL and at 1.25 µg/mL showed the fastest wound scratch closure.
- The mechanism was the upregulation of the phosphorylation of the PI3K/AKT signalling pathway for CFAC-3 1.25 µg/mL.
- Molecular docking showed a good binding affinity of CFAC-3 compounds towards AKT and ERK2.

GRAPHICAL ABSTRACT

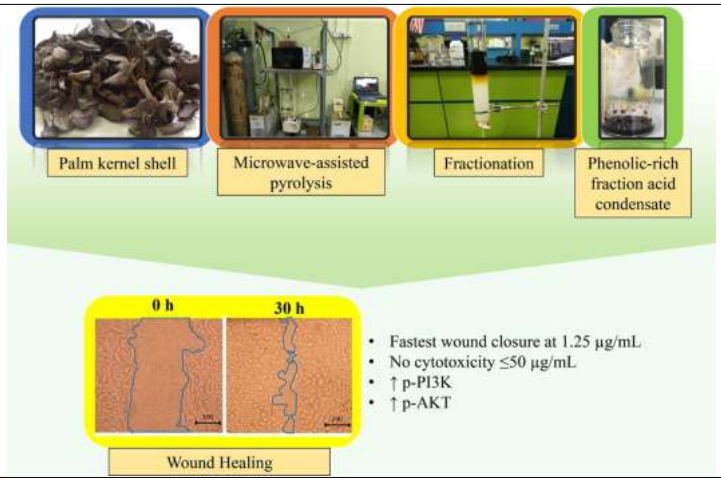

ARTICLE INFO

Article history:
Received 23 July 2022
Received in revised form 7 August 2022
Accepted 8 August 2022
Published 1 September 2022

Keywords:
Biomass
Phenolic-rich acid condensate
Antioxidant
Cytotoxicity
Wound healing
Palm kernel shell

ABSTRACT

Biomass valorisation is conventionally associated with the production of green biofuels. However, this could extend beyond the conventional perception of biomass application into other domains such as medical sciences. Acid condensate (AC) obtained from pyrolysis promises a good potential for biomedical applications, notably for its antimicrobial, antioxidant, and anti-inflammatory properties. In this study, concentrated AC extract (CACE) obtained from microwave-assisted pyrolysis of palm kernel shells was fractionated, and the resulting fractions were pooled according to similar thin layer chromatography profiles into combined fractions (CFACs). CFACs were evaluated for total phenolic content, antioxidant level, cytotoxicity, and wound healing activities toward human skin fibroblast cells (HSF 1184). CFAC-3 showed the highest total phenolic content (624.98 ± 8.70 µg GAE/mg of sample) and antioxidant activities (DPPH IC_{50} of 29.47 ± 0.74 µg/mL, ABTS of 1247.13 ± 27.89 µg TE/mg sample, FRAP of 24.26 ± 0.71 mmol Fe(II)/mg sample, HFRS of 257.74 ± 1.74 µg/mL) compared to CACE (DPPH IC_{50} of 81.76 ± 2.81 µg/mL, ABTS of 816.95 ± 30.49 µg TE/mg sample, FRAP of 9.22 ± 0.66 mmol Fe(II)/mg sample, HFRS of 689.30 ± 36.00 µg/mL), no cytotoxic properties at ≤50 µg/mL, and significantly faster wound closure (at 1.25 µg/mL) compared to the control 12 h after treatment. The phosphorylation of the phosphatidylinositol 3-kinase (PI3K) and protein kinase B (AKT) were upregulated, thus indicating that wound healing of CFAC-3 followed through this signalling pathway. To conclude, phenolic-rich CFAC-3 obtained from the pyrolysis of palm kernel shells demonstrated potential biomedical application as an alternative wound healing agent with high antioxidant and wound-healing activity. To the best of our knowledge, this was the first study to report on the wound healing activity of AC and its wound healing mechanism.

* Corresponding author at: Tel.: +60-7-5530652
E-mail address: zainulakmar@utm.my

Please cite this article as: Mohd Hamzah M.A.A., Hasham R., Nik Malek N.A.N., Hashim Z., Yahayu M., Abdul Razak F.I., Zakaria Z.A. Beyond conventional biomass valorisation: pyrolysis-derived products for biomedical applications. Biofuel Research Journal 35 (2022) 1648-1658. DOI: 10.18331/BRJ2022.9.3.2

Contents

Abbreviations

ABTS	2,2′-Azino-bis(3-ethylbenzothiazoline-6-sulfonic acid)
AC	Acid condensate
AKT	Protein kinase B
BHA	Butylated hydroxyanisole
CACE	Concentrated AC extract
CFAC	Combined fraction AC
ERK	Extracellular signal-regulated kinase
DMEM	Dulbecco's Modified Eagle Medium
DPPH	2,2-Diphenyl-1-picrylhydrazyl
FRAP	Ferric reducing antioxidant power
GAE	Gallic acid equivalent
HFRS	Hydroxyl free radical scavenging
HSF	Human skin fibroblast
MTT	3-(4,5- Dimethyl-2-thiazolyl)-2, 5-diphenyl- 2*H*-tetrazolium bromide
PI3K	Phosphatidylinositol 3-kinase
ROS	Reactive oxygen species
TPC	Total phenolic content

1. Introduction

Malaysia produces around 19 million tonnes of palm oil annually, the second largest in the world. However, at the same time, a huge amount of solid and liquid oil palm biomass is also generated, which amounts to more than 140 million tonnes (Malaysian-German Chamber of Commerce and Industry, 2017). Improper disposal of the high volume of biomass waste through open burning or being left for natural degradation poses serious environmental problems as it may lead to the emission of greenhouse gases such as carbon dioxide and methane and cause air pollution (Purnomo et al., 2018).

Biomass valorisation into biofuels and value-added products offers a highly attractive solution for waste management, simultaneously reducing fossil fuel usage and the production of greenhouse gases (Yang et al., 2021). The advantages of biomass include carbon-neutrality, renewability, and sustainability in terms of not interfering with food and feed supplies. Biomass valorisation can be achieved *via* thermochemical conversions such as microwave-assisted pyrolysis, which yields biochar, bio-oil, acid condensate (AC), and syngas. Many research works focus on producing biofuel through biomass pyrolysis to achieve a low carbon-intensive environment. This offers the opportunity to utilise the other value-added products generated through this biomass valorisation pathway, i.e., biochar and AC.

AC is a reddish-brown pyrolytic liquid condensate obtained from the pyrolysis of highly lignocellulosic biomass such as palm kernel shells and is rich in phenol and its derivatives (Zulkifli et al., 2021). AC has been reported for various chemical and biological properties such as antioxidant (Zulkifli et al., 2021), antibacterial (Mohd Hamzah et al., 2022), antifungal (Ibrahim et al., 2013), and anti-inflammatory (Rabiu et al., 2021). In addition, AC has low cytotoxicity at a 100-fold dilution (Kimura et al., 2002), while some reported the range was between 0.14 to 2% v/v (Filippelli et al., 2021; Ho et al., 2021). It also does not pose a severe environmental hazard (Tiilikkala et al., 2010). Currently, the market size for AC is relatively small and valued at USD 4.5 million in 2019 and projected to grow to USD 6.4 million by 2027 as it is commercially used in agriculture such as pesticide and fertiliser and animal feed as a feed supplement. A recent study has incorporated AC in an oral application to prevent biofilm formation related to dental caries (de Souza et al., 2021).

Chronic wounds are a big burden on the health care system due to their prevalence and high-cost projections, with recent estimates at USD 96.8 billion (Sen, 2021). In Malaysia, surgical site infection incidence at public hospitals was 11.7% which was higher than published figures from India (5%) and Greece (5.3%) (Wong and Holloway, 2019). Bad management of microbial infection can, in turn, lead to prolonged healing and, worse, becoming non-healing wounds due to a longer inflammation phase (Rowan et al., 2015). In recent years, one-third of the drugs intended for wound healing have been obtained or derived from plants (Lordani et al., 2018) due to their potent antimicrobial and wound-healing properties while exhibiting fewer side effects.

Please cite this article as: Mohd Hamzah M.A.A., Hasham R., Nik Malek N.A.N., Hashim Z., Yahayu M., Abdul Razak F.I., Zakaria Z.A. Beyond conventional biomass valorisation: pyrolysis-derived products for biomedical applications. Biofuel Research Journal 35 (2022) 1648-1658. DOI: 10.18331/BRJ2022.9.3.2

In light of the above, this work aimed to evaluate the cell cytotoxicity and wound-healing activities of phenolic-rich fractions of AC extract obtained through the pyrolysis of palm kernel shells towards human skin fibroblast (HSF 1184). Moreover, to the best of our knowledge, the *in vitro* wound-healing activity and wound-healing mechanism of AC compounds were also investigated for the first time.

2. Materials and Methods

2.1. Sample preparation of palm kernel shell

The palm kernel shell samples were obtained from a local palm oil mill located in Johor, Malaysia. The sample was washed using tap water, sun-dried for 3 d, and grounded (Df-25 automatic herb grinder, DA DE Brand) to 1-3 mm before use (Zulkifli et al., 2021).

2.2. Production of acid condensate

Concentrated AC extract (CACE) was produced using a laboratory-scale microwave-assisted pyrolysis reactor setup previously described by Abas et al. (2018). AC production was performed based on the optimisation study using response surface methodology *via* Design Expert Software Version 7 on three different factors. From the study, the highest yield of AC was recorded at 29.1 wt% and was achieved at the following optimized conditions; nitrogen flow rate of 3 L/min, microwave power of 575 W, and final temperature of 450 ºC (Zulkifli et al., 2021). The obtained AC was collected, filtered, and extracted using ethyl acetate (EA) AR grade at a 1:1 ratio (Loo et al., 2008). The AC extracts were then concentrated using a rotary evaporator (120 mBar, 80ºC, Heidolph, Germany), dried in a desiccator, and termed CACE.

2.3. Fractionation of acid condensate

The CACE was fractionated using column chromatography (5 cm i.d. × 80 cm) with silica gel (0.063-0.200 mm, Merck, Germany) as stationary phase and increasing polarity solvent system of *n*-hexane, ethyl acetate, and methanol as mobile phase. The 134 different fractions collected were pooled based on the similarity of the thin layer chromatography profile. Nine combined fractions (termed as CFAC 1-9) were obtained; fraction 10-11 (CFAC-1), fraction 12-16 (CFAC-2), fraction 17-24 (CFAC-3), fraction 25-32 (CFAC-4), fraction 33-40 (CFAC-5), fraction 41-45 (CFAC-6), fraction 46-59 (CFAC-7), fraction 60-94 (CFAC-8), and fraction 95-134 (CFAC-9).

2.4. Total phenolic content

The total phenolic content (TPC) in AC was determined as follows (Ma et al., 2014); 1 mL of the CFACs and 1 mL of 50% of Folin Ciocalteu reagent were mixed, followed by the addition of 1 mL of 10% sodium carbonate (105.99 g/mol, QRec). The mixture was left to stand for 2 h at room temperature, and the absorbance was measured at 765 nm using a UV-vis spectrophotometer (Shimadzu UV-1800, Japan). Similar procedures were repeated for gallic acid as standard. The determined TPC was expressed as µg gallic acid equivalent/mL of dried sample (µg GAE/mL).

2.5. Antioxidant activity

The 2,2-diphenyl-1-picrylhydrazyl (DPPH) assay was performed with minor modifications to the method described by Brand-Williams et al. (1995), where 1 mL of CFAC-3 was mixed with 2 mL of methanolic DPPH reagent. The mixture was shaken at 100 rpm and allowed to stand at room temperature for 30 min. The absorbance was measured at 517 nm with methanol as blank. The ferric reducing antioxidant power (FRAP) assay was conducted according to Ma et al. (2014) by adding 100 µL of 30 µg/mL CFAC-3 or standard L(+)-Ascorbic acid and butylated hydroxyanisole (BHA) 96%, respectively, into 3 mL of freshly mixed FRAP reagent (300 mM acetate buffer (pH 3.6), 10 mM 2,4,6-tripyridyl-s-triazine dissolved in 40 mM hydrochloric acid, and 20 mM ferric chloride in the ratio of 10:1:1) and shaken thoroughly before being left upright to react for 90 min at 37 ºC in the dark. The absorbance of the mixture was recorded at 593 nm using a UV-vis spectrophotometer. The results were expressed as mmol Fe(II) being reduced by per milligram of the sample (mmol Fe(II)/mg sample). The 2,2'-azino-bis(3-ethylbenzothiazoline-6-sulfonic acid) radical scavenging (ABTS) assay was carried out as described by Re et al. (1999). ABTS radical cation was prepared by mixing both 7 mM ABTS solution and 4.9 mM potassium persulphate solution in a 1:1 ratio (v/v). The radical stock solution of ABTS•+ was diluted using ethanol to an absorbance of 0.8 ± 0.005 at 734 nm. The Trolox solution was used to generate the Trolox standard curve. CFAC-3 or standards (L(+)-ascorbic acid and butylated hydroxyanisole) with a volume of 0.4 mL (20 µg/mL) was mixed with 3.6 mL of the ABTS•+ solution and incubated at 37 °C for 7 min followed by measurement at 734 nm.

2.6. Cell cytotoxicity study

Cell cytotoxicity assay was performed using MTT (3-(4,5- Dimethyl-2-thiazolyl)-2, 5-diphenyl- 2*H*-tetrazolium bromide) assay procedure described by Mustaffa et al. (2015) with a slight modification. The fibroblast cells were seeded in 96-well microplates at a density of 5×10^5 cells/well with 100 µL of Dulbecco's Modified Eagle Medium (DMEM) containing 10% v/v foetal bovine serum (complete DMEM) and incubated overnight at 37 °C in a humidified atmosphere containing 5% CO_2 to allow the cells to confluence in the wells. Then, the medium was discarded and replaced with 100 µL complete DMEM containing 0.1% v/v DMSO of different concentrations of 100, 50, 25, 12.5, 6.25, and 3.125 µg/mL of CFAC-3 in respective wells. The wells without treatment served as a negative control. The plate was incubated for 24 and 48 h at 37 °C in a humidified atmosphere containing 5% CO_2. After incubation, the cell was washed with 100 µL phosphate buffer saline. Sterile MTT solution of 5 mg/mL was added by 20 µL to each well, incubated for 3 h, replaced with 200 µL of DMSO to each well, and left at room temperature for 30 min to allow the insoluble formazan to dissolve. The absorbance of the supernatant was measured at 570 nm using an ELISA microplate reader. The percentage cell viability was calculated using **Equation 1**.

$$\text{Cell viability} = Abs_{570}\,(\text{treated cells}) / Abs_{570}\,(\text{control cells}) \times 100 \qquad \text{Eq. 1}$$

2.7. Scratch wound healing assay

The scratch wound healing assay was carried out using the method by Mustaffa et al. (2015). The fibroblast cells were grown at a density of 5×10^5 cells/well in a 6-well plate and cultured in complete DMEM for 24 h. The fibroblast cells with 90% confluency underwent starvation by replacing the current media with DMEM without foetal bovine serum for 24 h. After 24 h, the media was removed, the confluence cells were scratched using the sterilized pipette tip (yellow tips; volume 100 µL), washed with 1 mL sterile phosphate buffer saline, and treated with 2 mL of 0.1% v/v DMSO in complete DMEM media (as negative control) and CFAC-3 with a concentration of 1.25 µg/mL and 12.5 µg/mL for 30 h. The pictures of wound closure were taken at intervals of 0, 12, 24, and 30 h. The percentage of wound closure was calculated using **Equation 2**.

$$\text{Wound closure (\%)} = (\text{wound area at X h} - \text{wound area at 0 h}) / \text{wound area at 0 h} \times 100 \qquad \text{Eq. 2}$$

where X is 0, 12, 24, and 30 h.

2.8. Molecular docking

Autodock Vina (Trott and Olson, 2010) was used to evaluate the possible binding mode between CFAC-3 compounds and the specified binding site of target proteins (AKT, 3QKK and ERK2, 6NBS). The molecular docking was performed according to the method described by Rabiu et al. (2021) with slight modification. For protein 3QKK, grid box parameters used were X = 22.727, Y = −8.909, and Z = -5.768 and grid box dimensions were set at 20 × 20 × 20 Aº which covers all the amino acids in the binding site of PHLPP as reported by Zheng et al. (2022). For protein 6NBS, the parameters used were slightly modified based on Zheng et al. (2022), with coordinates for the X, Y, and Z axis at -12.806, -4.765, and 52.46, respectively, and dimensions for the grid box were 26 × 26 × 26 Aº. Ten best poses were generated for each ligand and scored using Autodock Vina

Please cite this article as: Mohd Hamzah M.A.A., Hasham R., Nik Malek N.A.N., Hashim Z., Yahayu M., Abdul Razak F.I., Zakaria Z.A. Beyond conventional biomass valorisation: pyrolysis-derived products for biomedical applications. Biofuel Research Journal 35 (2022) 1648-1658. DOI: 10.18331/BRJ2022.9.3.2

scoring functions. The docked complex forming hydrogen bond (H bond) and other non-covalent interactions was analysed by BIOVIA Discovery Studio Visualizer v19.1.0.18287.

2.9. Western blot

The phosphorylation level of phosphatidylinositol 3-kinase (PI3K) and protein kinase B (AKT) in HSF 1884 was determined using the method proposed by Abate et al. (2020) with modifications. Cell lysing was carried out using the Total Protein Extraction Maxi Kit (Cat. No. BC3710, SolarBio, China). The gel was loaded with 50 µg/well of SDS-cell lysate samples. The following primary antibodies, obtained from Cusabio, China, were used: phosphorylated (p)-PI3K Y607 (1:500, No. CSB-PA000712), p-Akt1 S246 (1:500, No. CSB-PA000465), anti-phospho-PI3K (1:1000, No. CSB-PA003767), anti-phospho-AKT (1:1000, No. CSB-PA000851), and anti-ACTB (1:1000, No. CSB-PA000350). The membranes were incubated with alkaline phosphatase-conjugated secondary antibody (A3687, Sigma-Aldrich, USA) at 1:10000 in 3% w/v bovine serum albumin. BCIP/NBT solution (BCIP/NBT Chromogen Kit, Cat. No. PR 1100, SolarBio, China) was used for protein band detection. The quantification of relative band densities was performed by scanning densitometry using ImageJ software (National Institute of Health, Bethesda, MD, USA). The grey intensity of p-PI3K/PI3K and p-AKT/AKT was calculated by **Equation 3**.

$$\text{Phosphorylated band ratio} = \text{phosphorylated band} / \text{unphosphorylated band} \times 100 \quad \text{Eq. 3}$$

2.10. Gas chromatography-mass spectrometry analysis

CFAC-3 were analysed for chemical compositions using a gas chromatograph-mass spectrometer (GC-MS, QP500, Shimadzu) based on the method suggested by Zhai et al. (2015) with slight modification. Briefly, a sample volume of 20 µL was dissolved in 2 mL of 95% methanol HPLC grade and filtered using a 0.2 µm membrane syringe filter. About 1 µL of the filtered sample was injected with a split rate of 20:1 into the capillary column (HP-5) with a length × diameter of 29.4 m × 0.25 mm. The injector pressure and split flow rate were 10.97 psi and 23.8 mL/min, respectively. Helium gas was used as a carrier gas at a flow rate of 2 mL/min, and the temperature of the injector was at 300 °C; 50 °C for 2 min with a heating rate of 10 °C/min up to 300 °C. The final temperature of around 325 °C was held for 10 min, and each sample was run for around 37 min. As for mass spectrometry (MS), the electron ionization with 70eV was used to detect the mass fragment at a scan range between 50 to 550 m/z. The ion source temperature and transfer line were set at 200 °C and 300 °C, respectively. The GC peak areas were integrated, and the component identification was made by comparing the MS with standards and with a library search (National Institute of Standard and Technology (NIST), USA.

2.11. Statistical analysis

All experiments were carried out in triplicates. Quantitative data were analysed using Microsoft Office Excel and GraphPad Prism 7.0 (GraphPad Software, Inc.), and all the results were expressed as a mean ± standard deviation.

3. Results and Discussion

3.1. Total phenolic content

The total phenolic content of CACE and CFACs is presented in **Figure 1**. CFAC-3 exhibited the highest TPC of 625 ± 9 µg GAE/mg of sample followed by CFAC-2 (434 ± 2 µg GAE/mg) and CFAC-1 (344 ± 15 µg GAE/mg). All these combined fractions displayed significantly higher TPC ($p < 0.0001$) than CACE, standing at 296 ± 6 µg GAE/mg. The other combined fractions (CFAC-4 to CFAC-9) exhibited significantly lower TPC than CACE. Most of the phenolic compounds were eluted early due to the low polarity solvent system of n-hexane and ethyl acetate, which had a good elution effect on monophenols and derivatives (Wang et al., 2016). The high amount of TPC in the CACE was due to the high lignin content of the feedstock used, as phenol and derivatives were mainly generated from thermal degradation of lignin fraction, which is very high in palm kernel shells (Collard and Blin, 2014). The obtained TPC value of CACE was more favourable than the AC obtained from oil palm fibre (Abas et al., 2018) and pineapple waste biomass, i.e., 95.0 ± 1.1 µg GAE/mg (Mathew et al., 2015).

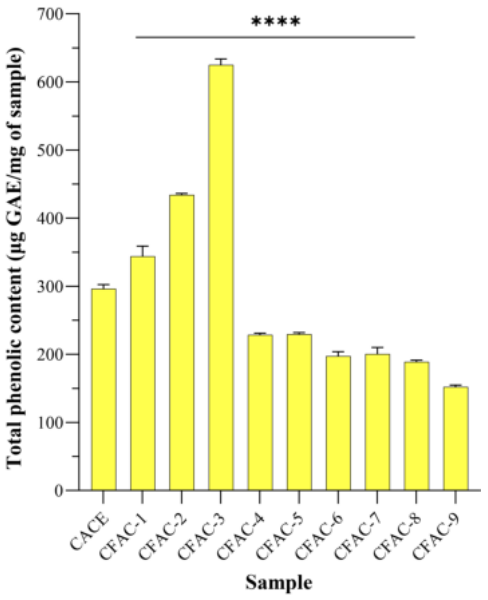

Fig. 1. Total phenolic content of concentrated acid condensate extract (CACE) and combined fraction acid condensate (CFAC) 1-9. Data from triplicate experiments are expressed as mean ± SD, ****$p < 0.0001$ compared with CACE.

3.2. Antioxidant activity

Reactive oxygen species (ROS) are closely related to wound healing, particularly inflammation- and oxidative stress-induced cellular damage, which is the main cause of delayed wound healing (Sanchez et al., 2018). Therefore, experimental studies on the regulation of ROS through antioxidant assays could be an important strategy for chronic wound healing. The results for the antioxidant assays of CACE and CFAC-3 are summarised in **Table 1**. CFAC-3 with IC_{50} of 29.5 ± 0.7 µg/mL exhibited significantly better DPPH radical scavenging activity than CACE ($p < 0.0001$) while showing similar scavenging activity to both standards of ascorbic acid and BHA with no statistical difference between them ($p > 0.05$). AC from walnut was reported to exhibit 1.5 times more DPPH radical scavenging activity than ascorbic acid (Wei et al., 2010).

Table 1.
Antioxidant activities of concentrated acid condensate extract (CACE) and combined fraction acid condensate (CFAC) determined by DPPH, ABTS radical scavenging activity, ferric reducing antioxidant power (FRAP), and hydroxyl free radical scavenging (HFRS) assays.

Antioxidant Assay	DPPH Radical Scavenging Activity, IC_{50} (µg/mL)	ABTS (µg TE/ mg sample)	FRAP	HFRS, IC_{50} (µg/mL)
CACE	81.76 ± 2.81*	816.95 ± 30.49	9.22 ± 0.66	689.30 ± 36.00
CFAC3	29.47 ± 0.74	1247.13 ± 27.89	24.26 ± 0.71	257.74 ± 1.74
BHA	29.63 ± 1.16	1575 ± 40.07	13.17 ± 0.18	-
Ascorbic acid	36.62 ± 1.34	148.99 ± 1.34	7.68 ± 0.17	152.09 ± 10.76

*Each value is expressed as a mean ± SD (n = 3)
Abbreviations: DPPH: 2,2-Diphenyl-1-picrylhydrazyl assay; ABTS: 2,2'-azino-bis (3-ethylbenzothiazoline-6-sulfonic acid) radical scavenging assay; FRAP: Ferric reducing antioxidant power; HFRS: Hydroxyl free radical scavenging assay; IC_{50}: Half-maximal inhibitory concentration.

Please cite this article as: Mohd Hamzah M.A.A., Hasham R., Nik Malek N.A.N., Hashim Z., Yahayu M., Abdul Razak F.I., Zakaria Z.A. Beyond conventional biomass valorisation: pyrolysis-derived products for biomedical applications. Biofuel Research Journal 35 (2022) 1648-1658. DOI: 10.18331/BRJ2022.9.3.2

AC from *Litchi chinensis* and rice hull showed lower or at least comparable scavenging activity to commercial antioxidant BHT (Kim et al., 2011; Yang et al., 2016). CFAC-3 displayed significantly higher ABTS radical scavenging activity ($p < 0.0001$) than CACE and ascorbic acid but not as good as BHA. Loo et al. (2008) reported that ABTS radical scavenging activity values of successfully isolated syringol, catechol, and 3-methylcatechol from *Rhizophora pyroligneous* acid were in the range of 956 ± 40 and 1039 ± 51 µg Trolox/mg sample.

CFAC-3 displayed the highest reducing ability towards TPTZ-Fe (III) with a FRAP value of 24.2 ± 0.7 mmol Fe(II)/mg sample ($p < 0.01$), followed by BHA, CACE, and ascorbic acid. Similar results were reported by Ma et al. (2014) and Wei et al. (2010), as AC from *Rosmarinus officinalis* and walnut had higher FRAP values than standard BHA and ascorbic acid. CFAC-3 exhibited better hydroxyl free radical scavenging (HFRS) activity with its IC_{50} value of 258 ± 2 µg/mL compared to CACE but lower activity compared to ascorbic acid as its IC_{50} was 1.69 times larger than that of ascorbic acid (152 ± 11 µg/mL). This finding aligned with the result reported by Wei et al. (2010), indicating that AC had a lower scavenging rate of hydroxyl free radical than ascorbic acid. All the findings showed a direct correlation between the TPC of AC and its antioxidant activities, strongly suggesting that the antioxidant activity was mainly attributed to the phenolic compounds as major compounds of AC. Theapparat et al. (2019) reported a similar correlation between the TPC of the AC obtained from the brushwood biomass waste of mangosteen, durian, rambutan, and langsat and DPPH radical scavenging activity.

3.3. Cell cytotoxicity

Cell cytotoxicity was determined through MTT dye colourimetric assay, which utilises cell metabolic activity as MTT is reduced by NAD(P)H-dependent cellular oxidoreductase and dehydrogenase enzymes in viable cells into water-insoluble purple formazan (Ghasemi et al., 2021). The cytotoxicity of CFAC-3 towards human skin fibroblast (HSF 1184) was rated based on the following guidelines suggested by Kanaparthy and Kanaparthy (2016); cell viability > 90% is non-cytotoxic, 60-90% is slightly cytotoxic, 30-60% is moderately toxic while less than 30% is strongly cytotoxic. The morphological alteration was observed when the concentration was increased to 50 µg/mL for CFAC-3. The cells exhibited shrinkage, became almost spherical and lost their ability to attach to the wall surface after 24 and 48 h incubation. These round shape cells were no longer living as they were detached, floated, and lifted from the material surface (Sani et al., 2017). These alterations were characteristic of apoptotic cell death and indicated the toxicity of the fraction at high concentrations (Diaz et al., 2011; Zhang et al., 2018).

Figure 2 shows the concentration effect of CFAC-3 on the percentage cell viability of human skin fibroblast (HSF 1184). CFAC-3 remained non-cytotoxic at a concentration of ≤50 µg/mL after 24 h. The percentage of cell viability significantly increased when treated with 12.5 µg/mL of CFAC-3 after 24 h, which displayed its ability to enhance cell proliferation. When the treatment period increased beyond 24 h, a concentration of 50 µg/mL started to pose slight cytotoxicity to the HSF 1184 after 48 h with a percentage cell viability of 67.7 ± 2.8% ($p < 0.001$), respectively. CFAC-3 became moderately cytotoxic at concentration of 100 µg/mL for 24 h (44.2 ± 13.6%, $p < 0.001$) and 75 µg/mL for 48 h (30.6 ± 10.0%, $p < 0.0001$). It was strongly cytotoxic to HSF 1184 at a concentration of 100 µg/mL after treatment for 48 h as the percentage cell viability significantly dropped ($p < 0.0001$) to 25.4 ± 7.9%.

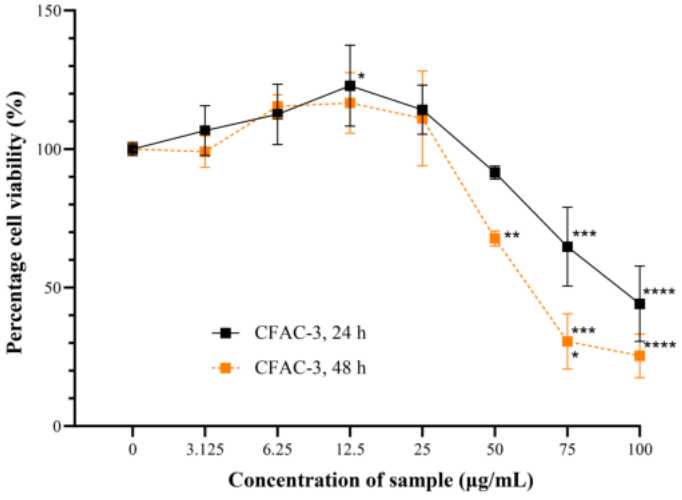

Fig. 2. Percentage cell viability of human skin fibroblast cell line (HSF 1184) after treatment with different concentrations (0, 3.125, 6.25, 12.5, 25, 50, 75 and 100 µg/mL) of combined fraction acid condensate 3 (CFAC-3) for the duration of 24 and 48 h. Data from triplicate biological experiments are expressed as mean ± SD, *$p < 0.05$, ***$p < 0.001$, ****$p < 0.0001$ compared with the control (0 h).

The fractionation process led to a lower range for safe and nontoxic concentration than CACE (≤100 µg/ml), which might be due to higher TPC in CFAC-3. Ho et al. (2013) revealed a similar result as the cell viability of RAW 264.7 cells was significantly reduced by the phenolic fraction of bamboo vinegar at a concentration ≥100 µg/mL after 24 h compared to bamboo vinegar extract, which remained non-cytotoxic 1% v/v. Mahmud et al. (2019) reported that the pyroligneous acid fraction with the highest phenolic content also showed moderate to strong cytotoxicity towards RAW 274.7 cells after 24 to 72 h of contact time (Mahmud et al., 2019). They also reported that at a concentration of ≤50 µg/mL, cell viability was ≥93.08% (after 24 h of contact time), while it was 85.90% for the concentration of 25 µg/mL after 72 h of exposure, indicating the tested compound`s non-cytotoxicity and slight cytotoxicity towards cells under the investigated conditions, respectively. Phenolic compounds such as trans-cinnamic acid and p-coumaric acid displayed similar cell viability towards fibroblast cells, where both compounds were found to be not toxic ≤300 µM (~50 µg/mL) (Viana et al., 2021).

CFAC-3 was observed to enhance proliferation of fibroblast cells at the concentration of 12.5 µg/mL ($p < 0.05$). At low concentrations, phenolic compounds can stimulate several signalling events, namely mitogen-activated protein kinases (MAPKs) and PI3K/AKT, which regulate cells functions, including proliferation, gene expression, differentiation, mitosis, cell survival, and apoptosis, while at high concentrations, ICE/Ced-3 proteases (caspases) is triggered, where this pathway plays a key role in apoptotic cell death (Kong et al., 2000; Abate et al., 2020). In short, AC can be biphasic, where at low concentration, it can cause cell proliferation, while at high concentration, it can be antiproliferative.

3.4. In vitro wound healing activity

The ability of CFAC-3 to stimulate fibroblast cell migration was observed at two concentrations with 10-fold differences (1.25 µg/mL and 12.5 µg/mL) under an inverted light microscope at time intervals of 0, 12, 24, and 30 h, as depicted in **Figure 3a**. Treatment with CFAC-3 (1.25 µg/mL) exhibited significantly fastest wound closure ($p < 0.01$ at 12 h, $p < 0.0001$ at 24 h, and $p < 0.001$ at 30 h) compared to the negative control after 30 h of treatment as shown in **Figure 3b**. This result opens a new perspective on applying AC as a wound healing agent. This finding also contradicted the previous report by Lee et al. (2011), indicating that oak wood vinegar exhibited antiproliferative activity against keratinocytes at a dose-dependent concentration (Lee et al., 2011). The difference in the results might be due to the high concentration of AC used in their study, which ranged up to 1.6%, while in this study, lower concentrations were used (1.25 and 12.5 µg/mL). This view was further supported by the experimental results where 12.5 µg/mL of CFAC-3 showed no cell migration, suggesting that low concentrations of CFAC-3 could promote wound healing activity while high concentrations could cause an antiproliferative effect instead. Phenolic derivatives from *Calendula arvensis* L., *Lavandula stoechas* L., and *Helichrysum italicum* extracts also showed enhanced wound healing activity at low concentrations of 1, 5, and 10 µL/mL of the sample after 24 h, 48 h, and 72 h of treatment, respectively (Addis et al., 2020).

Many phenolic derivatives have been reported to exhibit wound healing activity, including gallic acid, caffeic acid, ferulic acid, tyrosol, and hydroxytyrosol (Melguizo-rodríguez et al., 2021). hydroxytyrosol upregulates HO-1 expression through the PI3K/Akt and ERK1/2 pathways by stimulating the nuclear accumulation and stabilization of Nrf2, leading to the wound repair of vascular endothelial cells (Zrelli et al., 2015). Caffeic acid promotes wound healing through stimulation of collagen-like polymer

Please cite this article as: Mohd Hamzah M.A.A., Hasham R., Nik Malek N.A.N., Hashim Z., Yahayu M., Abdul Razak F.I., Zakaria Z.A. Beyond conventional biomass valorisation: pyrolysis-derived products for biomedical applications. Biofuel Research Journal 35 (2022) 1648-1658. DOI: 10.18331/BRJ2022.9.3.2

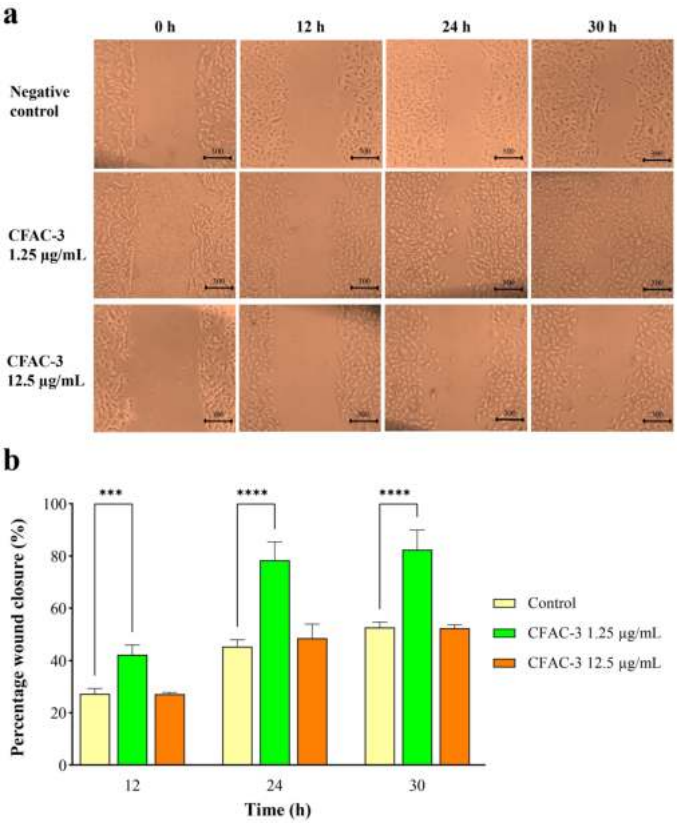

Fig. 3. *In vitro* scratch wound healing assay. **(a)** Scratch wound region of fibroblast cell observed under an inverted light microscope (4× magnification) at the time intervals of 0, 12, 24, and 30 h and **(b)** percentage of wound closure at time intervals of 12, 24, and 30 h after treatment with 0.1% DMSO medium (negative) and combined fraction acid condensate 3 (CFAC-3,1.25 and 12.5 µg/mL). Data from triplicate biological experiments are expressed as mean ± SD, *$p < 0.05$, **$p < 0.01$, ***$p < 0.001$, ****$p < 0.0001$.

synthesis in NIH 3T3 fibroblast cells while at the same time exhibiting anti-inflammatory activity such as myeloperoxidase activity, lipid peroxidation, and phospholipase A2 activity (Song et al., 2008). p-Coumaric acid and trans-cinnamic acid have been reported to enhance wound healing as both showed a 13-17% and 23-33% increase in migration compared to basal level wound closure of 8% (Viana et al., 2021). In short, CFAC-3 might stimulate ERK and PI3K/AKT signalling pathways which stimulate gene transcription involved in the proliferation and migration of cells, including fibroblasts (Lee et al., 2014; Zrelli et al., 2015).

3.5. Wound healing mechanism compounds via molecular docking verification

Molecular docking was performed to elucidate the potential molecular interaction of CFAC-3 towards AKT and extracellular signal-regulated kinase (ERK) enzymes. The hydrophobic motif (HFPQFpSYSAS) of AKT was targeted as it is the binding site of PH domain leucine-rich repeat protein phosphatase (PHLPP) on activated AKT and causes subsequent dephosphorylation on Ser473 leading to deactivation of AKT (Sierecki et al., 2010). The molecular docking target was specified to its D domain with a sequence of LEQYYDPSDEPVAEA of ERK2, thus preventing the dephosphorylation of ERK2 by MAPK phosphatases which downregulate the level of phosphorylated ERK2, thus reducing cell migration and proliferation (Tanoue et al., 2000; Bardwell et al., 2003)

The binding energy, as well as the formation of hydrogen bonds and other physical interactions towards AKT and ERK2, were determined for each ligand, as shown in **Table 2**. All the possible docking poses of selected CFAC-3 compounds showed negative binding energy indicating favourable binding affinity with the target enzymes. For AKT, most compounds displayed similar lowest binding energy, ranging from -4.0 to -5.5 kcal/mol. 1-butanone, 3-methyl-1-(2,4,6-trihydroxy-3-methylphenyl)- exhibited the lowest binding energy (-5.5 kcal/mol) while phenol, 2,6-dimethoxy- (-4.0 kcal/mol) showed the highest binding energy among the CFAC-3 compounds. The 3D mode and the 2D interaction residues of CFAC-3 compounds, i.e., 1-butanone, 3-methyl-1-(2,4,6-trihydroxy-3-methylphenyl)- with AKT at the hydrophobic motif (HFPQFpSYSAS) are illustrated in **Figure 4a**. All the ligands were observed to anchor in the binding pocket of the hydrophobic motif by mainly interacting with Arg144, Val145, Phe217, and Asp473. Besides that, other amino acid residues of the hydrophobic motif, including His468, Phe469, Pro470, Gln471, Phe472, Tyr474, and Ser475, non-covalently interacted with the ligands through a conventional hydrogen bond, carbon-hydrogen bond, pi-donor hydrogen bond, pi-alkyl, amide-pi stacked, alkyl and van der Walls as listed in **Table 2**.

Peptides derived from sea cucumber reportedly accelerated wound healing by upregulating ERK/AKT pathway by inhibiting the hydrophobic motif of AKT (Zheng et al., 2022). The highly important residue of Asp473 was generally targeted by the ligands as this residue is phosphomimetics, the phosphorylated Ser473 of activated AKT, which is the main target of the PHLPP for dephosphorylation of AKT (Balasuriya et al., 2018). The interaction between these amino acids and ligands would competitively inhibit PHLPP binding with AKT and interrupt the dephosphorylation. These results were in line with the western blotting assay as the p-AKT level remained high after being treated with CFAC-3 for 24 h.

For ERK, CFAC-3 compounds displayed similar lowest binding energy ranging from -3.9 to -5.4 kcal/mol. Based on the data tabulated in **Table 2**, 7,9-di-tert-butyl-1-oxaspiro(4,5)deca-6,9-diene-2,8-dione exhibited the lowest binding energy (-5.4 kcal/mol) while Ethanone, 1-(4,5-diethyl-2-methyl-1-cyclopenten-1-yl)- (-3.9 kcal/mol) showed the least favourable binding affinity among the CFPA-3 compounds. The 3D mode and the 2D interaction residues of the CFPA-3 compound with ERK2 at the D domain are illustrated in **Figure 4b**. In natural mitogen-activated protein kinase phosphatase (MKP)-ERK2 complex, MKP bound to the D domain of ERK2 by interacting with Asp 316 and Asp 319 to dephosphorylate and inactivate ERK2, and the failure of MKP interacting with Asp316 and Asp319 would interrupt the interaction of MKP and ERK2 (Tanoue et al., 2000). The docking results indicated that all CFPA-3 compounds occupied the binding site of MKP, which is a highly acidic patch of ERK2 consisting of residues Glu79, Tyr126, Asp160, Asp316, and Asp319 (Liu et al., 2006). The binding bonds of CFPA-3 were mainly conventional hydrogen bond, carbon-hydrogen bond, pi-pi T-shaped, pi-alkyl, alkyl and van der Walls. Interestingly, CFPA-3 compounds, except for 7,9-di-tert-butyl-1-oxaspiro(4,5)deca-6,9-diene-2,8-dione anchored to the D domain of ERK2, and interacted with Asp 316 and Asp 319 directly, which inhibited the binding of MKP to ERK2 and interrupted the dephosphorylation and inactivation of ERK2. Based on the molecular docking approach, CFAC-3 compounds were viable in targeting both AKT and ERK2.

3.6. Wound healing mechanism via PI3K/AKT pathway signalling – in vitro study

Western blotting experiments were performed to investigate the effects of CFAC-3 treatment (1.25 and 12.5 µg/mL) on the wound healing mechanism focusing on the protein expression and phosphorylation of PI3K and AKT of fibroblast cells. PI3K/AKT signalling pathway is a recognised pathway strongly associated with the formation of an epidermis barrier and wound healing as it regulates cell proliferation, differentiation, and migration, along with angiogenesis and metabolism (Hou et al., 2019; Qu et al., 2021). AKT is located as one of the target proteins downstream of PI3K. The activation of PI3K leads to the formation of phosphatidylinositol (3,4,5)-trisphosphate (PIP_3) from phosphorylation of phosphatidylinositol (3,4,5)-bisphosphate (PIP_2), which in turn leads to activation of AKT by phosphorylating serine residue of AKT. In this study, the total protein of unphosphorylated PI3K (t-PI3K), phosphorylated PI3K (p-PI3K), unphosphorylated AKT protein (t-AKT), and phosphorylated AKT protein (p-AKT) were detected and analysed using western blot in the presence of housekeeping protein β-Actin as a loading control at 4, 6, and 24 h intervals as shown in **Figure 5a** and **Figure 6a**. The relative protein quantification of p-PI3K/t-PI3K and p-AKT1/t-AKT1 as normalized to β-Actin was presented as a bar chart in **Figure 5b** and **Figure 6b** based on the grey value detection using ImageJ software.

Please cite this article as: Mohd Hamzah M.A.A., Hasham R., Nik Malek N.A.N., Hashim Z., Yahayu M., Abdul Razak F.I., Zakaria Z.A. Beyond conventional biomass valorisation: pyrolysis-derived products for biomedical applications. Biofuel Research Journal 35 (2022) 1648-1658. DOI: 10.18331/BRJ2022.9.3.2

Table 2.
Molecular docking of combined fraction acid condensate (CFAC3) compounds towards AKT (3QKK) and ERK (6NBS) enzymes in terms of lowest binding energy, formation of hydrogen bond (H bond), and other physical interactions.

Compound	AKT (3QKK)			ERK2 (6NBS)		
	BE (kcal/mol)	H Bond	Other interactions	BE (kcal/mol)	H Bond	Other interactions
1,2-Benzenediol, 3-methyl-	-4.1	***Conventional*** Tyr474 ***Pi-Donor H bond*** Val145	***Amide-Pi Stacked*** Asp473 ***Pi-Alkyl*** Arg144	-4.7	***Conventional*** Tyr129, Asp319	***Pi-Pi T-shaped*** Tyr129
Phenol, 2,6-dimethoxy-	-4.0	***Conventional*** Arg144, Val145 ***Carbon H bond*** Phe472, Tyr474	***Alkyl*** Val145 ***Pi-Alkyl*** Arg144	-4.9	***Conventional*** Tyr129. Arg133, Asp319 ***Carbon H bond*** Asn80	***Pi-Pi T-shaped*** Tyr129
3,5-Dimethoxy-4-hydroxytoluene	-4.9	***Conventional*** Ser216, Tyr474 ***Carbon H bond*** Phe472	***Amide-Pi Stacked*** Asp473 ***Alkyl*** Arg144 ***Pi-alkyl*** Arg144, Val145	-4.7	***Conventional*** Tyr126, Tyr129, Asp319 ***Carbon H bond*** Gln130, Tyr314	***Pi-PI T-Shaped*** Tyr129 ***Pi-alkyl*** Tyr126
Ethanone, 1-(4,5-diethyl-2-methyl-1-cyclopenten-1-yl)-	-4.3	***Conventional*** Val145	***Alkyl*** Ag144	-3.9	***Conventional*** Tyr126	***Pi-Alkyl*** Tyr129
1-Butanone, 3-methyl-1-(2,4,6-trihydroxy-3-methylphenyl)-	-5.5	***Conventional*** Arg144, Val145, Phe472 ***Pi-donor H bond*** Arg144	***Pi-Alkyl*** His468	-5.1	***Conventional*** Tyr126, Tyr129, Arg133, Asp319 ***Carbon H bond*** Arg133	***Pi-Pi T-Shaped*** Tyr129
7,9-Di-tert-butyl-1-oxaspiro(4,5)deca-6,9-diene-2,8-dione	-5.0	***Conventional*** Arg144	***Alkyl*** Arg144	-5.4	***Conventional*** Arg133	***Pi-Alkyl*** Tyr126

Abbreviations: BE: Binding energy; H Bond: hydrogen bond.

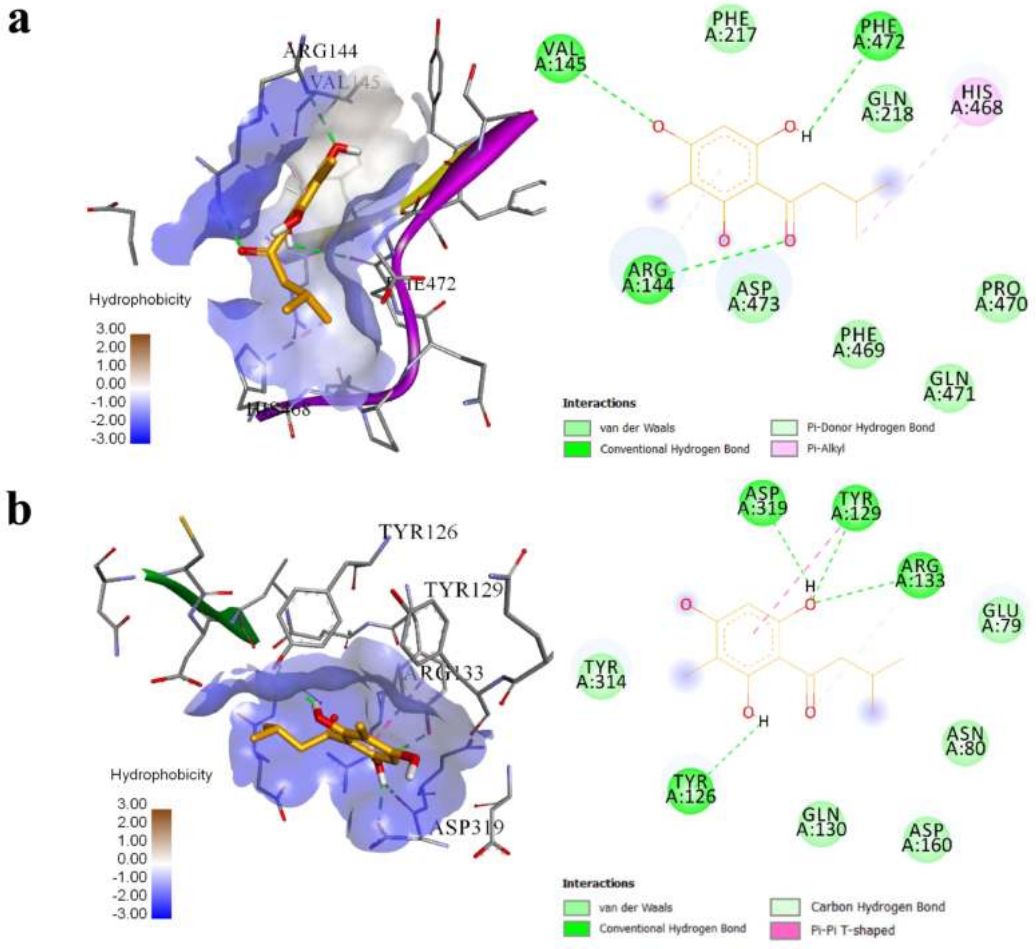

Fig. 4. 3D mode and 2D interaction of non-covalent interaction of 1-butanone, 3-methyl-1-(2,4,6-trihydroxy-3-methylphenyl)- with **(a)** AKT (3QKK) and **(b)** ERK2 (6NBS).

Please cite this article as: Mohd Hamzah M.A.A., Hasham R., Nik Malek N.A.N., Hashim Z., Yahayu M., Abdul Razak F.I., Zakaria Z.A. Beyond conventional biomass valorisation: pyrolysis-derived products for biomedical applications. Biofuel Research Journal 35 (2022) 1648-1658. DOI: 10.18331/BRJ2022.9.3.2

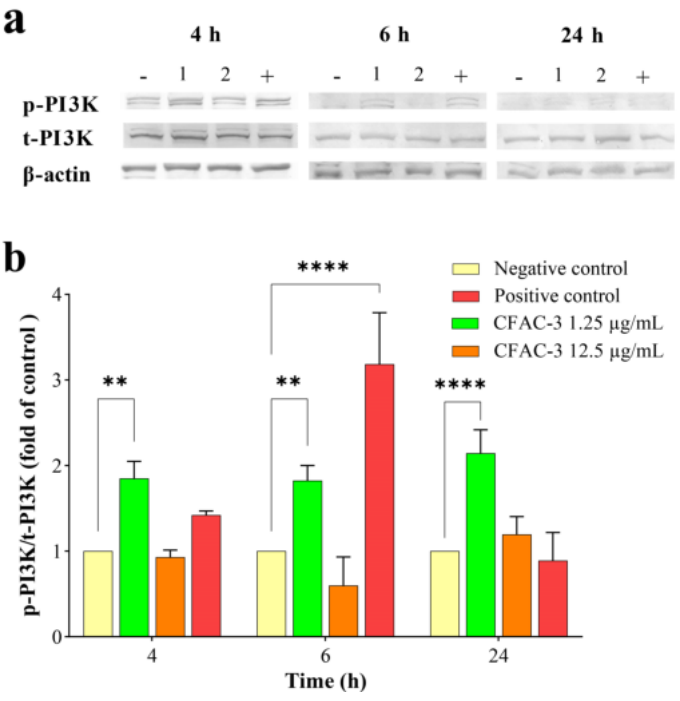

Fig. 5. PI3K phosphorylation. **(a)** Representative western blot showing protein levels of total and phosphorylated PI3K extracted from fibroblast cells after treatment with negative control (0.1% DMSO medium, -), combined fraction acid condensate 3 (CFAC-3 1.25 µg/mL (1) and 12.5 µg/mL (2)), and positive control (10 nM PDGF-BB, +) for 4, 6, and 24 h. **(b)** Bars represent the relative protein quantification of p-PI3K/t-PI3K normalized to β-Actin. Data are presented as the mean ± SD, $^{**}p < 0.01$, $^{****}p < 0.0001$ compared with the negative control.

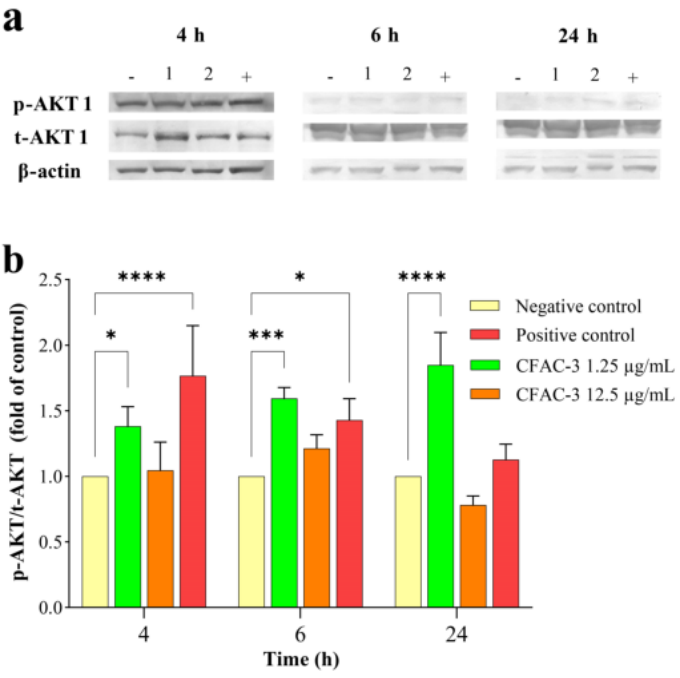

Fig. 6. AKT1 phosphorylation. **(a)** Representative western blot showing protein levels of total and phosphorylated AKT1 extracted from fibroblast cells with the negative control (0.1% DMSO medium, -), combined fraction acid condensate 3 (CFAC-3 1.25 µg/mL (1) and 12.5 µg/mL (2)), and positive control (10 nM PDGF-BB, +) for 4, 6, and 24 h. **(b)** Bars represent the relative protein quantification of p-AKT1/t-AKT1 normalized to β-Actin. Data from triplicate biological experiments are expressed as mean ± SD, $^{*}p < 0.05$, $^{**}p < 0.01$, $^{****}p < 0.0001$ compared with negative control.

The protein expression of t-PI3K and t-AKT remained relatively the same compared to the negative control after treatment at any time intervals, as shown in **Figure 5a** and **Figure 6a**. There was neither upregulation nor downregulation of protein expression after the treatment. To prevent the inaccuracy of the amount of protein loading, housekeeping protein β-Actin was used as an internal control for protein loading as well as a reference (western blot normalisation) in the western blotting analysis. The housekeeping protein β-Actin depicted a similar size and intensity of bands which showed that the amount of protein loaded onto SDS-PAGE gel was relatively the same, and the change in the band of p-PI3K and p-AKT was caused by the amount of protein phosphorylation. Meanwhile, the bands of p-PI3K and p-AKT showed a difference in terms of size and band intensity as the cells treated with 1.25 µg/mL CFAC-3 and positive control displayed darker and slightly thicker bands compared to the negative control. CFAC-3 treatment showed two opposite results. At the lower concentration of 1.25 µg/mL, relative p-PI3K/PI3K level showed significant increase compared to the negative control for all time intervals of 4 h ($p < 0.01$), 6 h ($p < 0.01$), and 24 h ($p < 0.0001$) while p-AKT/AKT level of 1.25 µg/mL CFAC-3 showed significant increase compared to negative control for all time intervals of 4 h ($p < 0.05$), 6 h ($p < 0.001$), and 24 h ($p < 0.0001$). Contrastingly, the treatment with 12.5 µg/mL of CFAC-3 yielded a decrease of p-PI3K/PI3K in HSF 1184 fibroblast cells compared with those in control cells at 6 h. Treatment with 12.5 µg/mL of CFAC-3 yielded no significant change in p-AKT/AKT level in fibroblast cells compared with those in negative control at other time intervals. Positive control showed significant increase of p-PI3K/PI3K level after 6 h ($p < 0.0001$) and p-AKT/t-AKT level after 4 h and 6 h ($p < 0.05$).

Thus, in this study, the treatment of CFAC-3 was able to upregulate the protein expression of p-PI3K and p-AKT as early as 4 h and maintained it until 24 h while there was no change to the protein expression of t-PI3K and t-AKT. This result is consistent with previous studies, which suggested that the phosphorylation of PI3K and Akt signalling pathways plays an important role in the promotion of proliferation and migration of fibroblasts, keratinocytes, and endothelial cells (Pericacho et al., 2013; Sepe et al., 2013). Treatment of dracorhodin perchlorate, a polyphenol, activated PI3K/AKT, ERK, p38/MAPK, and Wnt/β-catenin signalling cascades as there was a markedly increase in the phosphorylation level of p-AKT, p-ERK, and p-p38 in keratinocytes cells (HaCaT) (Lu et al., 2021). 4-hydroxylbenzylaldehyde treatment significantly increased phosphorylation of ERK and AKT in keratinocytes, leading to keratinocyte cell migration (Kang et al., 2017). Buxuahuayu decoction, which is a mixture of herbs containing polyphenols, was reported to regulate the level of nitric oxide (NO) in local wounds by activating the PI3K/Akt/eNOS signalling pathway when tested *in vivo* on rats with diabetic ulcers (Qu et al., 2021).

The treatment of CFAC-3 yielded two contrasting results at two different concentrations; low concentration (1.25 µg/mL) yielded upregulation of protein expression level of p-PI3K and p-AKT while high concentration (12.5 µg/mL) caused downregulation of the protein expression level. This finding shows that CFAC-3 exhibited a biphasic effect which means the increase or decrease of concentration of the drugs/chemicals could result in opposite effects (Kong et al., 2000). 3-hydroxytyrosol, the main component in olive oil, has been reported to be pro-angiogenesis at concentrations lower than 10 µM or approximately 1.5 µg/mL, which is similar to the concentration used in this study (Abate et al., 2020). Resveratrol has been reported to be anti-angiogenic as it inhibited AKT and ERK1/2 signalling pathways as the concentration increased from 25 to 100 µM to treat renal cell carcinoma cells (Zhao et al., 2018).

3.7. Gas chromatography-mass spectrometry analysis

Six chemical compounds were detected from the GC-MS analysis of CFAC-3, with phenol and derivatives representing the major compound group (93.2%). This group is mainly comprised of phenol, 2,6-dimethoxy-, known as syringol (46.1%) and 3,5-dimethoxy-4-hydroxytoluene (40.8%), followed by 6.3% of 1,2-benzenediol, 3-methylbenzenes. Phenol and derivatives as major constituents of AC were also reported by other researchers (Zhai et al., 2015; Mahmud et al., 2019). The high yield of phenol and derivatives can be attributed to the high lignin content (48.5 ± 0.6 wt%) of palm kernel shells (Wang et al., 2009). Most hydrocarbons

Please cite this article as: Mohd Hamzah M.A.A., Hasham R., Nik Malek N.A.N., Hashim Z., Yahayu M., Abdul Razak F.I., Zakaria Z.A. Beyond conventional biomass valorisation: pyrolysis-derived products for biomedical applications. Biofuel Research Journal 35 (2022) 1648-1658. DOI: 10.18331/BRJ2022.9.3.2

were removed when non-polar n-hexane was used as a solvent system (Wang et al., 2016). Besides these phenolic derivatives, ketones were also profiled including ethanone, 1-(4,5-diethyl-2-methyl-1-cyclopenten-1-yl)- (2.95%), 1-butanone, 3-methyl-1-(2,4,6-trihydroxy-3-methylphenyl)- (2.04%), and 7,9-di-tert-butyl-1-oxaspiro(4,5)deca-6,9-diene-2,8-dione (1.79%).

3.8. Limitations of the present study

The study was performed only using fractionated samples of AC extract that exhibited the highest TPC and antioxidant activities. The mass concentration of the samples used was based on the consistent dry weight of the sample. Molecular docking was performed based on a single compound to target enzyme interaction. Moreover, the *in vitro* wound healing mechanism was limited to phosphorylation of the PI3K/AKT signalling pathway at the molecular level.

4. Conclusions, practical implications, and future perspectives

4.1. Conclusions

CFAC-3 exhibited higher antioxidant activity compared to CACE and standards, which, based on the TPC and GC-MS analysis, could be associated with the presence of many phenolic compounds and their derivatives. It also showed no cytotoxicity at the concentration of ≤50 µg/mL against HSF 1184 after 24 h. CFAC-3 at a 1.25 µg/mL concentration led to the fastest wound closure. Molecular docking analysis suggested favourable binding energy for all chemical compounds present in CFAC-3, notably 7,9-di-tert-butyl-1-oxaspiro(4,5)deca-6,9-diene-2,8-dione, ethanone, and 1,2-benzenediol, 3-methyl- towards AKT and ERK2. This was further supported by the Western blot analysis as the treatment with 1.25 µg/mL CFAC-3 caused an upregulation of PI3K and AKT phosphorylation as soon as 4 h.

4.2. Practical implications of the study

To the best of the authors` knowledge, this is the first report to determine the wound healing activity of phenolic-rich fraction of AC from palm kernel shell and its potential wound healing mechanism through the PI3K/AKT signalling pathway. These findings broadened the application of bioproducts obtained from biomass valorization (through pyrolysis herein) beyond the conventional applications in biomedical science, particularly for wound healing.

4.3. Future perspectives

Further study using specific inhibitors of PI3K and AKT such as wortmannin is required to further confirm that CFAC-3 directly targeted these proteins. *In vivo* study using rats would allow a more in-depth understanding of the wound healing effect of CFAC-3 in a more complex system which mimics the human system.

Acknowledgements

The authors acknowledged the financial support from Universiti Teknologi Malaysia (UTM) through the Research University Grant (07G78). We would also like to express our gratitude to UTM Digital Centre for its high-performance computing facilities.

References

[1] Abas, F.Z., Ani, F.N., Zakaria, Z.A., 2018. Microwave-assisted production of optimized pyrolysis liquid oil from oil palm fiber. J. Clean. Prod. 182, 404-413.

[2] Abate, M., Pisanti, S., Caputo, M., Citro, M., Vecchione, C., Martinelli, R., 2020. 3-Hydroxytyrosol promotes angiogenesis in vitro by stimulating endothelial cell migration. Int. J. Mol. Sci. 21(10), 3657.

[3] Addis, R., Cruciani, S., Santaniello, S., Bellu, E., Sarais, G., Ventura, C., Maioli, M., Pintore, G., 2020. Fibroblast proliferation and migration in wound healing by phytochemicals: evidence for a novel synergic outcome. Int. J. Med. Sci. 17(8), 1030-1042.

[4] Balasuriya, N., Kunkel, M.T., Liu, X., Biggar, K.K., Li, S.S.C., Newton, A.C., O'Donoghue, P., 2018. Genetic code expansion and live cell imaging reveal that Thr-308 phosphorylation is irreplaceable and sufficient for Akt1 activity. J. Biol. Chem. 293(27), 10744-10756.

[5] Bardwell, A.J., Abdollahi, M., Bardwell, L., 2003. Docking sites on MEKs, MAP kinase phosphatases, and the Elk-1 transcription factor compete for binding to ERK2 and are crucial for enzymatic activity. Biochem. J. 370, 1077-1085.

[6] Brand-Williams, W., Cuvelier, M.E., Berset, C., 1995. Use of a free radical method to evaluate antioxidant activity. LWT-Food Sci. Technol. 28(1), 25-30.

[7] Collard, F.X., Blin, J., 2014. A review on pyrolysis of biomass constituents: mechanisms and composition of the products obtained from the conversion of cellulose, hemicelluloses and lignin. Renew. Sust. Energy Rev. 38, 549-608.

[8] de Souza, J.L.S., Alves, T., Camerini, L., Nedel, F., Campos, A.D., Lund, R.G., 2021. Antimicrobial and cytotoxic capacity of pyroligneous extracts films of *Eucalyptus grandis* and chitosan for oral applications. Sci. Reports. 11(1), 1-10.

[9] Diaz, R., Quiles, M.T., Guillem-Marti, J., Lopez-Cano, M., Huguet, P., Ramon-Y-Cajal, S., Reventos, J., Armengol, M., Arbos, M.A., 2011. Apoptosis-like cell death induction and aberrant fibroblast properties in human incisional hernia fascia. Am. J. Pathol. 178(6), 2641-2653.

[10] Filippelli, A., Ciccone, V., Loppi, S., Morbidelli, L., 2021. Characterization of the safety profile of sweet chestnut wood distillate employed in agriculture. Safety. 7(4), 79.

[11] Ghasemi, M., Turnbull, T., Sebastian, S., Kempson, I., 2021. The MTT assay: utility, limitations, pitfalls, and interpretation in bulk and single-cell analysis. Int. J. Mol. Sci. 22(23), 12827.

[12] Ho, C.L., Lin, C.S., Li, L.H., Hua, K.F., Ju, T.C., 2021. Inhibition of pro-inflammatory mediator expression in macrophages using wood vinegar from griffith's ash. Chin. J. Physiol. 64(5), 232.

[13] Ho, C.L., Lin, C.Y., Ka, S.M., Chen, A., Tasi, Y.L., Liu, M.L., Chiu, Y.C., Hua, K.F., 2013. Bamboo vinegar decreases inflammatory mediator expression and NLRP3 inflammasome activation by inhibiting reactive oxygen species generation and protein kinase C-α/δ activation. PLoS One. 8(10), e75738.

[14] Hou, B., Cai, W., Chen, T., Zhang, Z., Gong, H., Yang, W., Qiu, L., 2019. Vaccarin hastens wound healing by promoting angiogenesis via activation of MAPK/ERK and PI3K/AKT signaling pathways *in vivo*. Acta Cirúrgica Bras. 34.

[15] Ibrahim, D., Kassim, J., Sheh-Hong, L., Rusli, W., 2013. Efficacy of pyroligneous acid from *Rhizophora apiculata* on pathogenic *Candida albicans*. J. Appl. Pharm. Sci. 3(7), 007-013.

[16] Kanaparthy, A., Kanaparthy, R., 2016. Cytotoxicity of endodontic sealers-a comparative study using L-929 mouse skin fibroblast cell response-an ex-vivo study. Int. J. Med. Res. Health Sci. 5(1), 59-62.

[17] Kang, C.W., Han, Y.E., Kim, J., Oh, J.H., Cho, Y.H., Lee, E.J., 2017. 4-Hydroxybenzaldehyde accelerates acute wound healing through activation of focal adhesion signalling in keratinocytes. Sci. Rep. 7(1), 1-11.

[18] Kim, S.P., Yang, J.Y., Kang, M.Y., Park, J.C., Nam, S.H., Friedman, M., 2011. Composition of liquid rice hull smoke and anti-inflammatory effects in mice. J. Agric. Food Chem. 59(9), 4570-4581.

[19] Kimura, Y., Suto, S., Tatsuka, M., 2002. Evaluation of carcinogenic/co-carcinogenic activity of Chikusaku-eki, a bamboo charcoal by-product used as a folk remedy, in BALB/c 3T3 cells. Biol. Pharm. Bull. 25(8), 1026-1029.

[20] Kong, A.N.T., Yu, R., Chen, C., Mandlekar, S., Primiano, T., 2000. Signal transduction events elicited by natural products: role of MAPK and caspase pathways in homeostatic response and induction of apoptosis. Arch. Pharm. Res. 23(1), 1-16.

[21] Lee, C.S., Yi, E.H., Kim, H.R., Huh, S.R., Sung, S.H., Chung, M.H., Ye, S.K., 2011. Anti-dermatitis effects of oak wood vinegar on the DNCB-induced contact hypersensitivity via STAT3 suppression. J. Ethnopharmacol. 135(3), 747-753.

Please cite this article as: Mohd Hamzah M.A.A., Hasham R., Nik Malek N.A.N., Hashim Z., Yahayu M., Abdul Razak F.I., Zakaria Z.A. Beyond conventional biomass valorisation: pyrolysis-derived products for biomedical applications. Biofuel Research Journal 35 (2022) 1648-1658. DOI: 10.18331/BRJ2022.9.3.2

[22] Lee, T.H., Lee, G.W., Park, K.H., Mohamed, M.A.A., Bang, M.H., Baek, Y.S., Son, Y., Chung, D.K., Baek, N.I., Kim, J., 2014. The stimulatory effects of *Stewartia koreana* extract on the proliferation and migration of fibroblasts and the wound healing activity of the extract in mice. Int. J. Mol. Med. 34(1), 145-152.

[23] Liu, S., Sun, J.P., Zhou, B., Zhang, Z.Y., 2006. Structural basis of docking interactions between ERK2 and MAP kinase phosphatase 3. Proc. Natl. Acad. Sci. 103(14), 5326-5331.

[24] Loo, A.Y., Jain, K., Darah, I., 2008. Antioxidant activity of compounds isolated from the pyroligneous acid, *Rhizophora apiculata*. Food Chem. 107(3), 1151-1160.

[25] Lordani, T.V.A., de Lara, C.E., Ferreira, F.B.P., de Souza Terron Monich, M., Mesquita da Silva, C., Felicetti Lordani, C.R., Giacomini Bueno, F., Vieira Teixeira, J.J., Lonardoni, M.V.C., 2018. Therapeutic effects of medicinal plants on cutaneous wound healing in humans: a systematic review. Mediators Inflammation. 2018, 7354250.

[26] Lu, C.C., Yang, J.S., Chiu, Y.J., Tsai, F.J., Hsu, Y.M., Yin, M.C., Juan, Y.N., Ho, T.J., Chen, H.P., 2021. Dracorhodin perchlorate enhances wound healing via β-catenin, ERK/p38, and AKT signaling in human HaCaT keratinocytes. Exp. Ther. Med. 22(2) 1-9.

[27] Ma, C., Li, W., Zu, Y., Yang, L., Li, J., 2014. Antioxidant properties of pyroligneous acid obtained by thermochemical conversion of *Schisandra chinensis* Baill. Molecules. 19(12), 20821-20838.

[28] Mahmud, K.N., Hashim, N.M., Ani, F.N., Zakaria, Z.A., 2019. Antioxidants, toxicity, and nitric oxide inhibition properties of pyroligneous acid from palm kernel shell biomass. Waste Biomass Valorization. 11(11), 6307-6319.

[29] Malaysian-German Chamber of Commerce and Industry, 2017. Oil palm biomass & biogas in Malaysia, 2017. EU-Malaysia Chamb. Commer. Ind.

[30] Mathew, S., Zakaria, Z.A., Musa, N.F., 2015. Antioxidant property and chemical profile of pyroligneous acid from pineapple plant waste biomass. Process Biochem. 50(11), 1985-1992.

[31] Melguizo-rodríguez, L., de Luna-Bertos, E., Ramos-torrecillas, J., Illescas-montesa, R., Costela-ruiz, V.J., García-martínez, O., 2021. Potential effects of phenolic compounds that can be found in olive oil on wound healing. Foods. 10(7), 1642.

[32] Mohd Hamzah, M.A.A., Hasham, R., Nik Malek, N.A.N., Raja Sulong, R.S., Yahayu, M., Abdul Razak, F.I., Zakaria, Z.A., 2022. Structural-based analysis of antibacterial activities of acid condensate from palm kernel shell. Biomass Convers. Biorefin.

[33] Mustaffa, N.A.A.W., Hasham, R., Sarmidi, M.R., 2015. An *in vitro* study of wound healing activity of *Ficus deltoidea* leaf extract. J. Teknol. 77(3), 67-72.

[34] Pericacho, M., Velasco, S., Prieto, M., Llano, E., López-Novoa, J.M., Rodríguez-Barbero, A., 2013. Endoglin haploinsufficiency promotes fibroblast accumulation during wound healing through Akt activation. PLoS One. 8(1), e54687.

[35] Purnomo, H., Okarda, B., Dewayani, A.A., Ali, M., Achdiawan, R., Kartodihardjo, H., Pacheco, P., Juniwaty, K.S., 2018. Reducing forest and land fires through good palm oil value chain governance. For. Policy Econ. 91, 94-106.

[36] Qu, K., Cha, H.J., Ru, Y., Que, H., Xing, M., 2021. Buxuhuayu decoction accelerates angiogenesis by activating the PI3K-Akt-eNOS signalling pathway in a streptozotocin-induced diabetic ulcer rat model. J. Ethnopharmacol. 273, 113824.

[37] Rabiu, Z., Hamzah, M.A.A.M., Hasham, R., Zakaria, Z.A., 2021. Characterization and antiinflammatory properties of fractionated pyroligneous acid from palm kernel shell. Environ. Sci. Pollut. Res. 28(30), 40535-40543.

[38] Re, R., Pellegrini, N., Proteggente, A., Pannala, A., Yang, M., Rice-Evans, C., 1999. Antioxidant activity applying an improved ABTS radical cation decolorization assay. Free Radical Biol. Med. 26(9-10), 1231-1237.

[39] Rowan, M.P., Cancio, L.C., Elster, E.A., Burmeister, D.M., Rose, L.F., Natesan, S., Chan, R.K., Christy, R.J., Chung, K.K., 2015. Burn wound healing and treatment: review and advancements. Crit. Care 19(1), 1-12.

[40] Sanchez, M.C., Lancel, S., Boulanger, E., Neviere, R., 2018. Targeting oxidative stress and mitochondrial dysfunction in the treatment of impaired wound healing: a systematic review. Antioxidants. 7(8), 98.

[41] Sani, N.S., Malek, N.A.N.N., Jemon, K., Kadir, M.R.A., Hamdan, H., 2017. Effect of mass concentration on bioactivity and cell viability of calcined silica aerogel synthesized from rice husk ash as silica source. J. Sol-Gel Sci. Technol. 82(1), 120-132.

[42] Sen, C.K., 2021. Human wound and its burden: updated 2020 compendium of estimates. Adv. Wound Care. 10(5), 281-292.

[43] Sepe, L., Ferrari, M.C., Cantarella, C., Fioretti, F., Paolella, G., 2013. Ras activated ERK and PI3K pathways differentially affect directional movement of cultured fibroblasts. Cell. Physiol. Biochem. 31(1), 123-142.

[44] Sierecki, E., Sinko, W., McCammon, J.A., Newton, A.C., 2010. Discovery of small molecule inhibitors of the ph domain leucine-rich repeat protein phosphatase (PHLPP) by chemical and virtual screening. J. Med. Chem. 53(19), 6899-6911.

[45] Song, H.S., Park, T.W., Sohn, U.D., Shin, Y.K., Choi, B.C., Kim, C.J., Sim, S.S., 2008. The effect of caffeic acid on wound healing in skin-incised mice. Korean J. Physiol. Pharmacol. 12(6), 343-347.

[46] Tanoue, T., Adachi, M., Moriguchi, T., Nishida, E., 2000. A conserved docking motif in MAP kinases common to substrates, activators and regulators. Nat. Cell Biol. 2(2), 110-116.

[47] Theapparat, Y., Khongthong, S., Rodjan, P., Lertwittayanon, K., Faroongsarng, D., 2019. Physicochemical properties and in vitro antioxidant activities of pyroligneous acid prepared from brushwood biomass waste of Mangosteen, Durian, Rambutan, and Langsat. J. For. Res. 30(3), 1139-1148.

[48] Tiilikkala, K., Fagernäs, L., Tiilikkala, J., 2010. History and use of wood pyrolysis liquids as biocide and plant protection product. Open Agric. J. 4, 111-118.

[49] Trott, O., Olson, A.J., 2010. AutoDock Vina: improving the speed and accuracy of docking with a new scoring function, efficient optimization, and multithreading. J. Comput. Chem. 31(2), 455-461.

[50] Viana, R.D.S., Aquino, F.L.T.D., Barreto, E., 2021. Effect of *trans*-cinnamic acid and *p*-coumaric acid on fibroblast motility: a pilot comparative study of *in silico* lipophilicity measure. Nat. Prod. Res. 35(24), 5872-5878.

[51] Wang, S., Wang, K., Liu, Q., Gu, Y., Luo, Z., Cen, K., Fransson, T., 2009. Comparison of the pyrolysis behavior of lignins from different tree species. Biotechnol. Adv. 27(5), 562-567.

[52] Wang, S., Wang, Y., Leng, F., Chen, J., Qiu, K., Zhou, J., 2016. Separation and enrichment of catechol and sugars from bio-oil aqueous phase. BioResources. 11(1), 1707-1720.

[53] Wei, Q., Ma, X., Zhao, Z., Zhang, S., Liu, S., 2010. Antioxidant activities and chemical profiles of pyroligneous acids from walnut shell. J. Anal. Appl. Pyrolysis. 88(2), 149-154.

[54] Wong, K.A., Holloway, S., 2019. An observational study of the surgical site infection rate in a General Surgery Department at a General Hospital in Malaysia. Wounds Asia. 2(2), 10-19.

[55] Yang, J.F., Yang, C.H., Liang, M.T., Gao, Z.J., Wu, Y.W., Chuang, L.Y., 2016. Chemical composition, antioxidant, and antibacterial activity of wood vinegar from *Litchi chinensis*. Molecules. 21(9), 1150.

[56] Yang, Q., Zhou, H., Bartocci, P., Fantozzi, F., Mašek, O., Agblevor, F.A., Wei, Z., Yang, H., Chen, H., Lu, X., Chen, G., Zheng, C., Nielsen, C.P., McElroy, M.B., 2021. Prospective contributions of biomass pyrolysis to China's 2050 carbon reduction and renewable energy goals. Nat. Commun. 12, 1698.

[57] Zhai, M., Shi, G., Wang, Y., Mao, G., Wang, D., Wang, Z., 2015. Chemical compositions and biological activities of pyroligneous acids from walnut shell. BioResources. 10(1), 1715-1729.

[58] Zhang, Y., Chen, X., Gueydan, C., Han, J., 2018. Plasma membrane changes during programmed cell deaths. Cell Res. 28(1), 9-21.

[59] Zhao, Y., Tang, H., Zeng, X., Ye, D., Liu, J., 2018. Resveratrol inhibits proliferation, migration and invasion via Akt and ERK1/2 signaling pathways in renal cell carcinoma cells. Biomed. Pharmacother. 98, 36-44.

[60] Zheng, Z., Li, M., Jiang, P., Sun, N., Lin, S., 2022. Peptides derived from sea cucumber accelerate cells proliferation and migration for wound healing by promoting energy metabolism and upregulating the ERK/AKT pathway. Eur. J. Pharmacol. 921, 174885.

Please cite this article as: Mohd Hamzah M.A.A., Hasham R., Nik Malek N.A.N., Hashim Z., Yahayu M., Abdul Razak F.I., Zakaria Z.A. Beyond conventional biomass valorisation: pyrolysis-derived products for biomedical applications. Biofuel Research Journal 35 (2022) 1648-1658. DOI: 10.18331/BRJ2022.9.3.2

[61] Zrelli, H., Kusunoki, M., Miyazaki, H., 2015. Role of hydroxytyrosol-dependent regulation of HO-1 expression in promoting wound healing of vascular endothelial cells *via* Nrf2 *De Novo* synthesis and stabilization. Phyther. Res. 29(7), 1011-1018.

[62] Zulkifli, S.E., Hamzah, M.A.A.M., Yahayu, M., Aziz, A.A., Hashim, N.M., Zakaria, Z.A., 2021. Optimisation of microwave-assisted production of acid condensate from palm kernel shell and its biological activities. Biomass Convers. Biorefin.

Dr Zainul Akmar Zakaria is an Associate Professor of Environmental Biotechnology at the School of Chemical and Energy Engineering, Faculty of Engineering, Universiti Teknologi Malaysia (UTM). He works on biomass valorization and microbial technology. He has an h-index of 21 on WoS and has published 2 Research Books, 9 Edited Books, and 16 Book Chapters. One of his research books was awarded the "National Book Award 2018" in the biochemistry category. Dr Zainul served as *Visiting Scientist* to Argentina and Mexico and as *Program Head* for the UTM-CONICET, Argentina R&D Program (2015-2018). His research profile on Scopus can be found at: https://www.scopus.com/authid/detail.uri?authorId=57219988588.

Dr Rosnani Hasham is a lecturer in the School of Chemical and Energy Engineering at Universiti Teknologi Malaysia (UTM). She has dedicated her research career to a broad range of areas, including skin molecular biology, novel ingredients discovery and formulation, and pharmacological evaluation. Rosnani is also a wellness and aromatherapy consultant and trainer. Dr Rosnani is an active researcher and passionate about exploring and studying Malaysian indigenous plants as a potent source of medicinal or cosmeceuticals by identifying their bioactive components. Her expertise also includes research and applications of nanomaterials and transdermal and controlled release evaluation. Her research profile is available at https://orcid.org/0000-0001-8389-9397.

Dr Zanariah Hashim is currently a Senior Lecturer in the School of Chemical and Energy Engineering, Faculty of Engineering, Universiti Teknologi Malaysia (UTM). She also serves as UTM's head of the Food and Biomaterial Engineering Research Group. She obtained her PhD from Osaka University, Japan, in metabolomics. She has published over 20 indexed research articles with a Scopus H-index of 7. Her main research interests include multivariate data analysis, chemometrics, and metabolite profiling. Her Scopus author ID is 56222817800, which may be found at https://orcid.org/0000-0001-9347-9951.

Dr Fazira Ilyana is a senior lecturer in the Department of Chemistry in the Faculty of Science, Universiti Teknologi Malaysia (UTM), Johor, Malaysia. She has a PhD in Organometallic and Computational Chemistry from Australian National University, Malaysia, in 2015. Her current research focuses on synthesising inorganic compounds and studying non-linear optical materials for second and third-order applications. She has published over 32 peer-reviewed journal papers with an h-index of 12, and her work has received over 456 citations. Her research profile on Google scholar can be found at the following link: https://scholar.google.com/citations?hl=en&user=jUgKAIUAAAAJ&view_op=list_works&sortby=pubdate.

Mohd Amir Asyraf Mohd Hamzah is a PhD researcher in the School of Chemical and Energy Engineering at Universiti Teknologi Malaysia (UTM). He has an M.Phil. degree in Chemistry from UTM and a Bachelor's Degree in Biotechnology from University College London, United Kingdom. His research interests include (1) pyrolysis product application and (2) microbial pigment. His research profile on Google Scholar can be found at the following link: https://scholar.google.com/citations?user=QCS9r5AAAAAJ&hl=en.

Assoc. Prof. Ts ChM Dr Nik Ahmad Nizam Nik Malek is the Director of the Centre for Sustainable Nanomaterials (CSNano), Ibnu Sina Institute for Scientific and Industrial Research (ISI-ISIR), Universiti Teknologi Malaysia (UTM) and associate professor at the Department of Biosciences, Faculty of Science, UTM. He received his PhD in chemistry from UTM in 2010. His research background is applied materials science for biological and medical applications. He is the chief editor of the Journal of Materials in Life Science and Proceedings of Science and Mathematics. He has published 76 indexed papers with an H-indexed of 16 and over 1000 citations. His research profile on Scopus can be found at: https://www.scopus.com/authid/detail.uri?authorId=35995651900.

Maizatulakmal Yahayu is currently a Senior Research Officer in the Analytical Unit at the Institute of Bioproduct Development (IBD), Universiti Teknologi Malaysia (UTM). She is also a training and short courses coordinator in IBD, a registered chemist from the Malaysian Institute of Chemistry (IKM), and a lifetime member of the Malaysian Natural Product Society (MNPS). Her research area focuses on herbal extraction, HPLC phytochemical profiling and utilization of agricultural biomass (particularly on the pyrolysis process). She has published over 20 papers in indexed journals with a Scopus h-index of 10. Her research profile on Scopus can be found at: https://www.scopus.com/authid/detail.uri?authorId=41662471300.

Please cite this article as: Mohd Hamzah M.A.A., Hasham R., Nik Malek N.A.N., Hashim Z., Yahayu M., Abdul Razak F.I., Zakaria Z.A. Beyond conventional biomass valorisation: pyrolysis-derived products for biomedical applications. Biofuel Research Journal 35 (2022) 1648-1658. DOI: 10.18331/BRJ2022.9.3.2